Magnetic Mapping of Battery Cells

Jarred Olson

April 23, 2026

Approved for public release. OTR 2026-00530.

Magnetic properties of material and electrochemical systems

1. Extent of electron pairing and spin manifests magnetic dipoles, whose long-range order within a material gives rise to Ferro-, Ferri-, and Paramagnetic domains

Ferromagnetism

Legend:

Local domain of a material

Magnetic Field vector

2. Right-hand curl rule: projection of a magnetic field (“B”) oriented perpendicular to electrical current (“I”) in operando

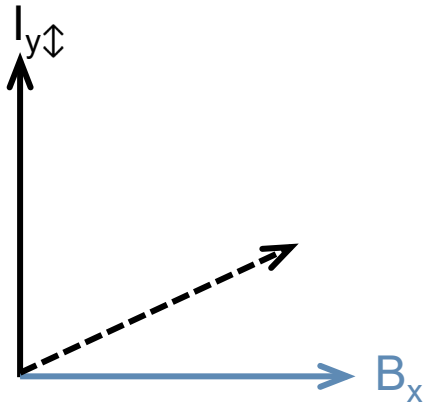

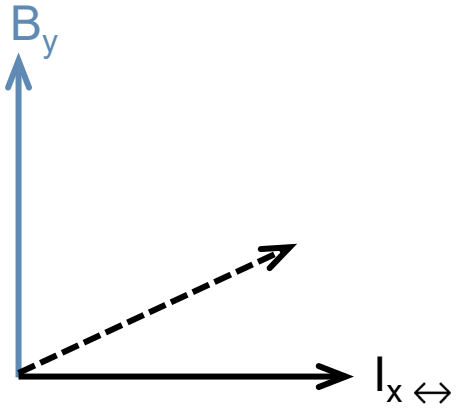

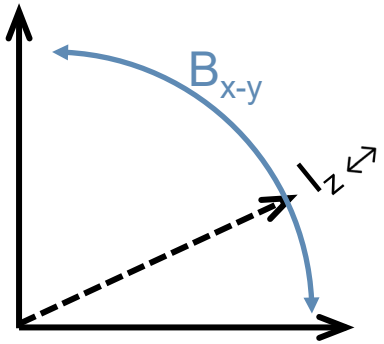

Magnetic fields of a material can be native or dynamically driven properties

Commercial, off-the-shelf magnetic field mapping systems can enable studies of Li-ion battery cells

Magnetic field mapper

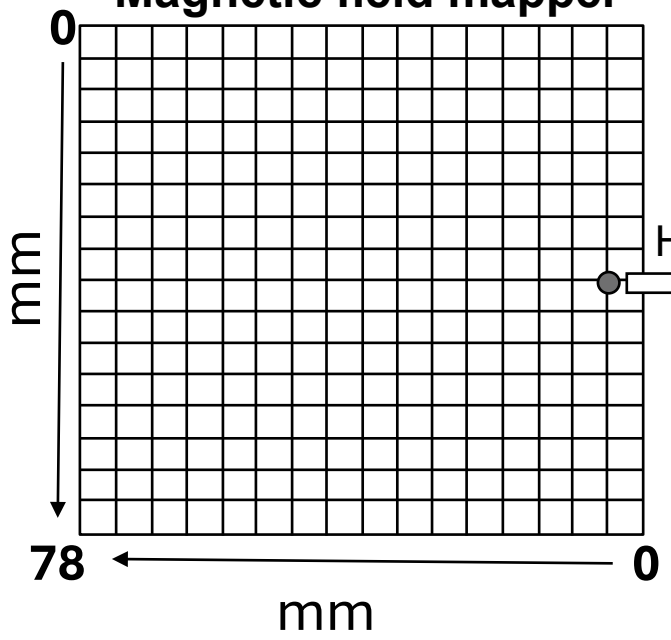

Hall effect magnetometer

Basic operating principle

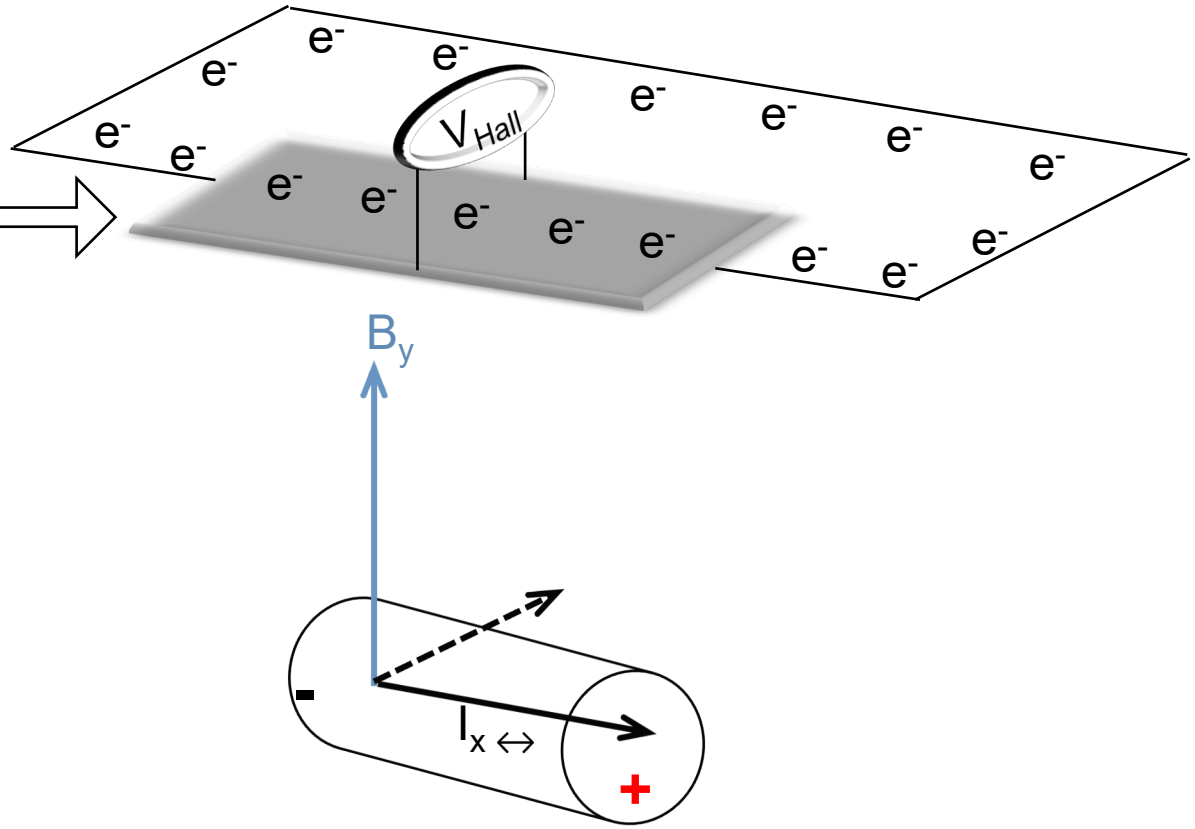

- Array of magnetometers across a grid
- Sensitivity: 4μT

Array of hall effect magnetometers can resolve vector-specific magnetic fields

Experimental details

Background signal of array

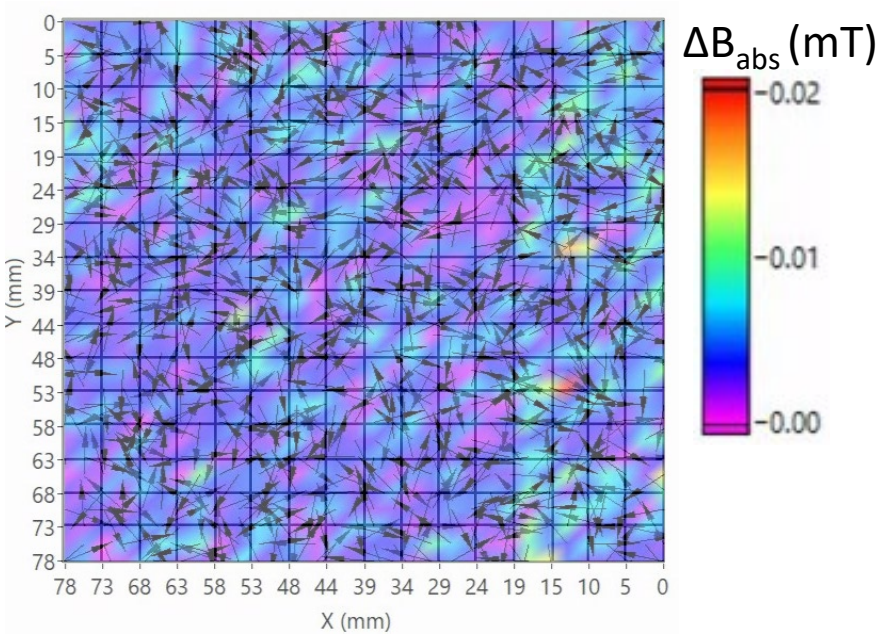

- Array of magnetometers across a grid
- Sensitivity: 4μT
- Cells placed directly upon array

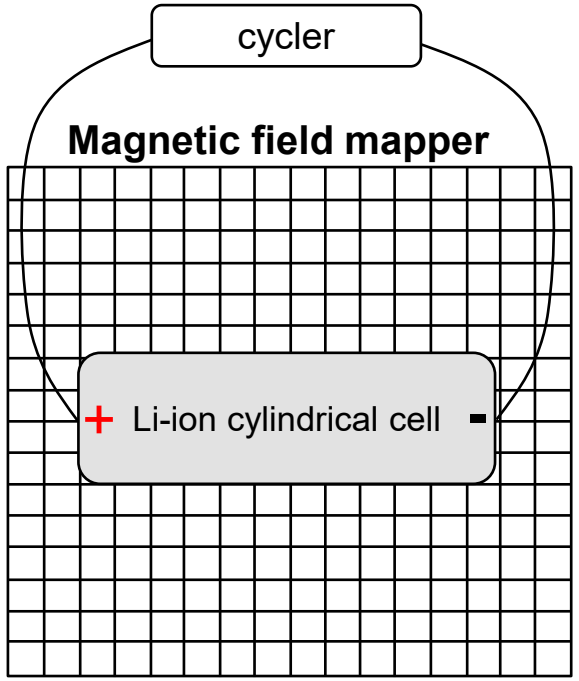

1) 3.5C CC-CV (~0.5C cut-off)
2) Rest at OCV
3) 3.5C CC discharge
4) Rest at OCV
5) Recharge to native SoC (30%)

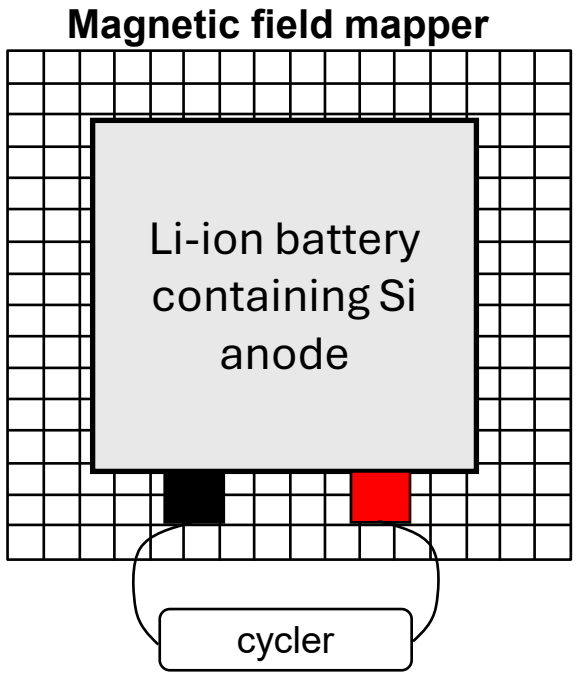

1) 1CC-CV (0.05C cut-off)
2) Rest at OCV
3) 1C CC discharge
4) Rest at OCV
5) Recharge to native SoC (30%)

Different material chemistries and cell geometries will be presented

Experimental coordinates

Background signal of array

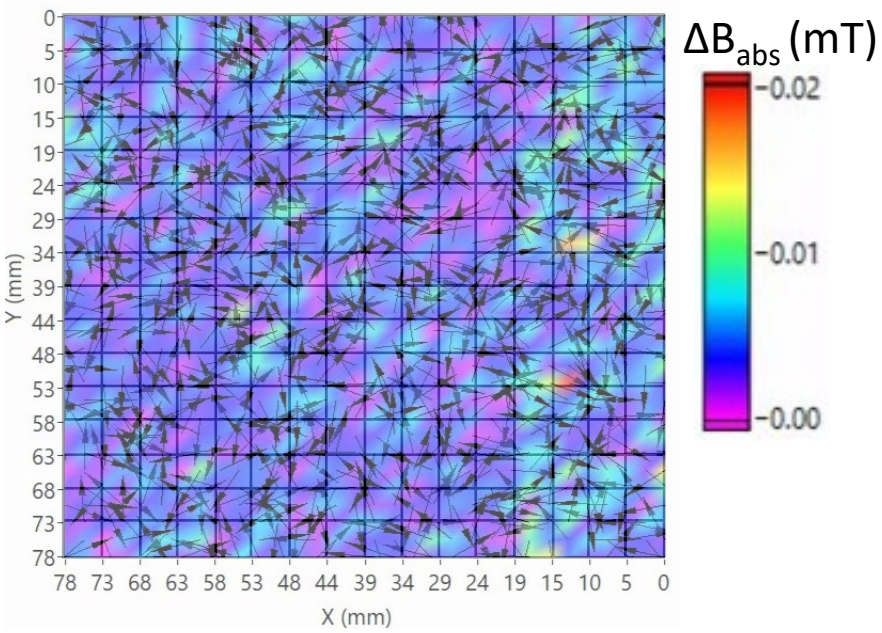

Experimental coordinates

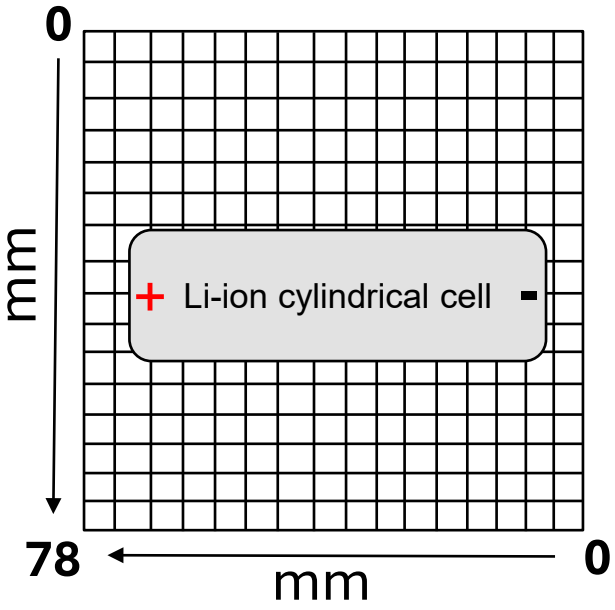

Experimental coordinates

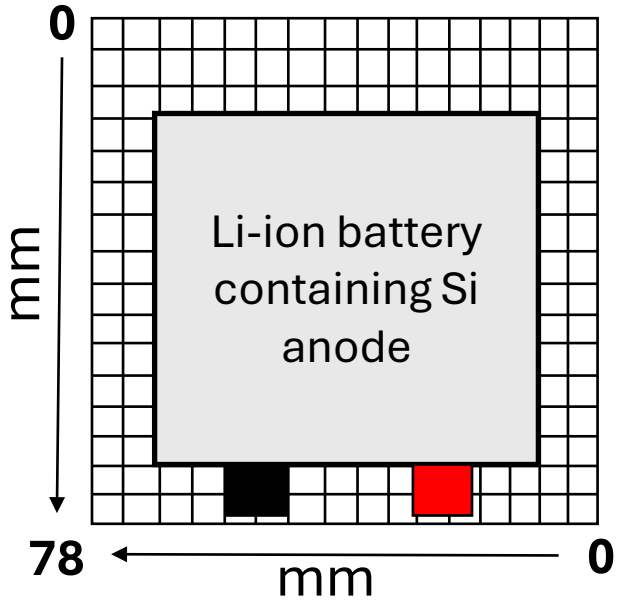

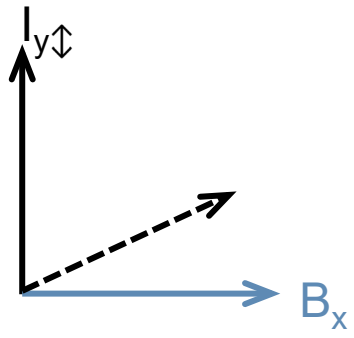

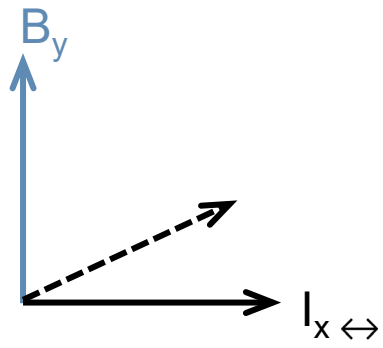

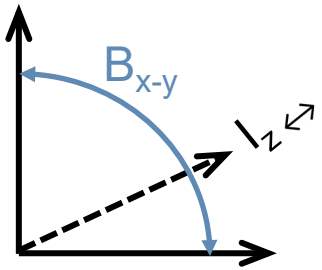

B_y field indicates current travels along cell length

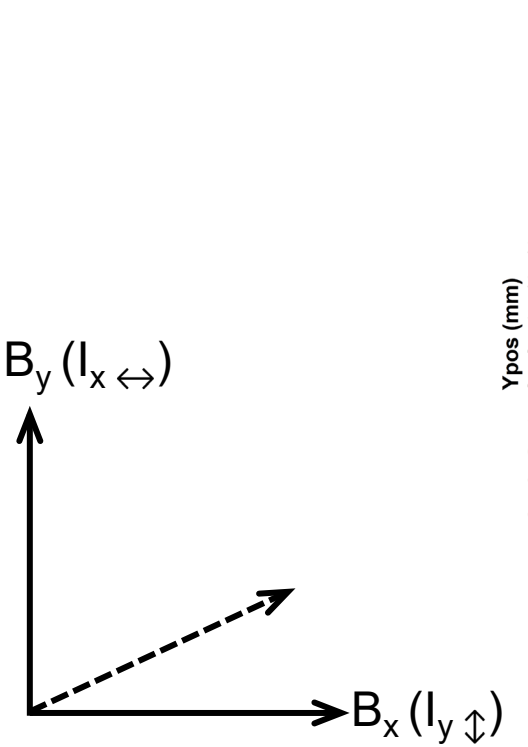

"snapshot" of vector-specific fields at 3.5V

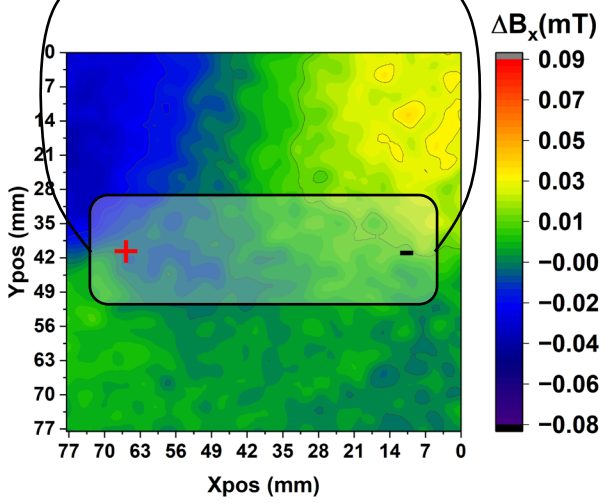

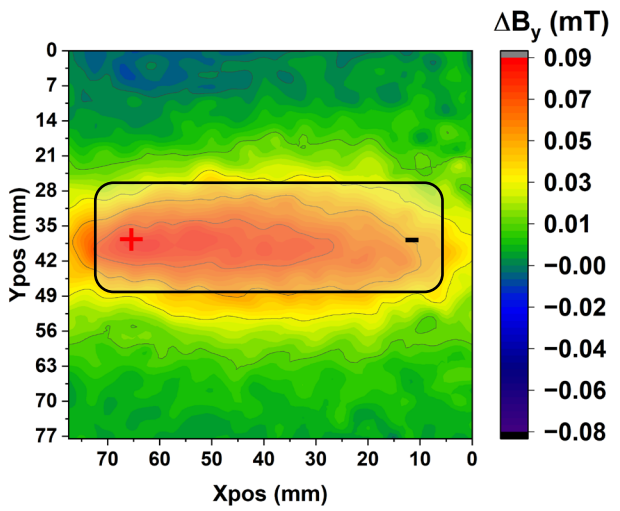

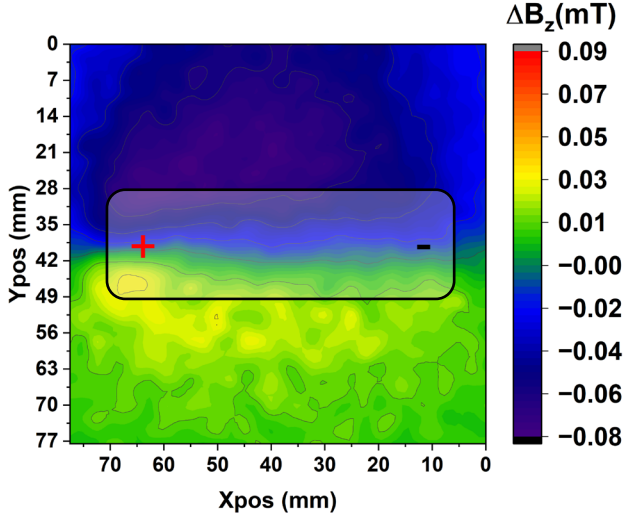

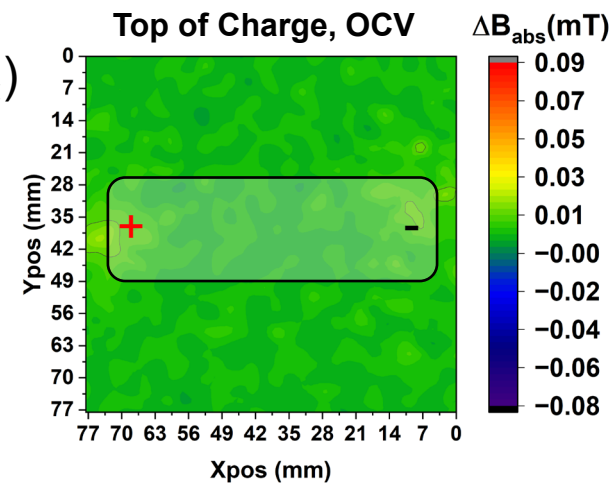

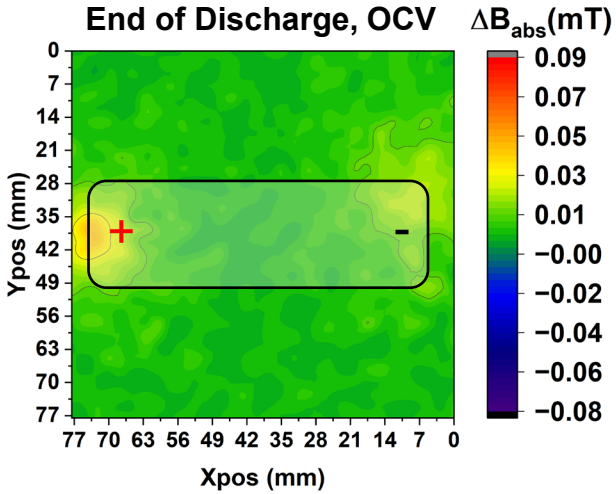

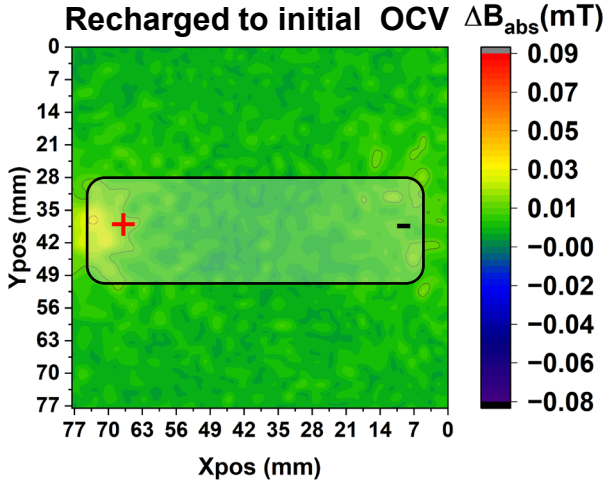

Initial findings reveal flux is greatest along length of cell, fraction remains at cell terminals during OCV and post-cycle

B_x fields are likely from cycler leads

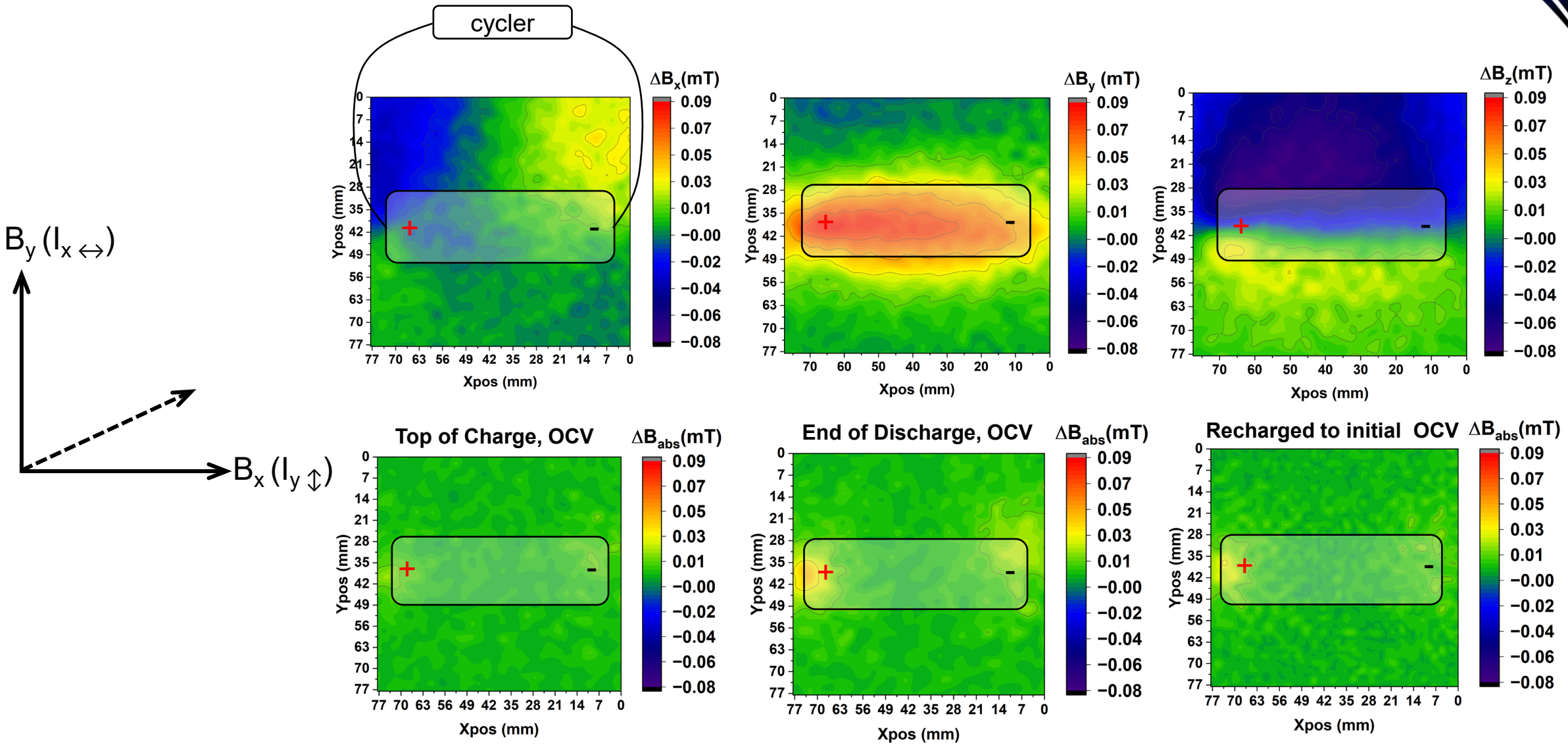

Initial findings reveal flux is greatest along length of cell, fraction remains at cell terminals during OCV and post-cycle

Si-containing pouch cells exhibit unique magnetic signatures as a function of State of Charge

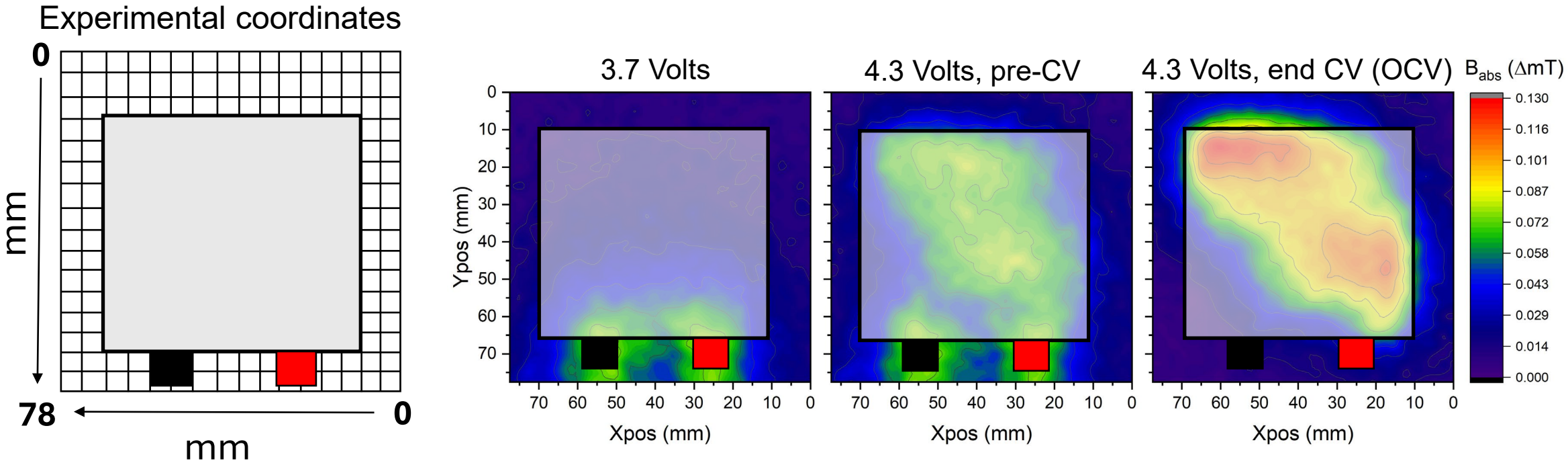

- Magnetic characteristics develop across cell during charge
- Magnetic field remains static at OCV

Field develops while passing current, remains at OCV

Why is this important for space vehicles and missions?

Budgeting for magnetic cleanliness

Unit	$\mu_{Alloc,DC}$ (mA-m^2)	*B* at 1 m (nT)	DC Allocations (A-m^2)		
			Materials	Magnets	Currents
Battery	394	78.8	227	227	227
Solar array*,a	435	87.1	308	n/a	308
Latch valves*	299	59.9	n/a§	299	n/a
Transponder	74	14.7	43	43	43
Power switching unit**	406	81.3	287	n/a	287
CIDP†	106	21.2	75	n/a	75
HPCA‡	444	88.9	314	n/a	314
EDI-GDU*	10	2.1	7.3	n/a	7.3
DES*	42	8.3	24	24	24

Russell, C.T., Anderson, B.J., Baumjohann, W. *et al.* The Magnetospheric Multiscale Magnetometers. *Space Sci Rev* **199**, 189–256 (2016)

Operational modes of batteries can induce torques

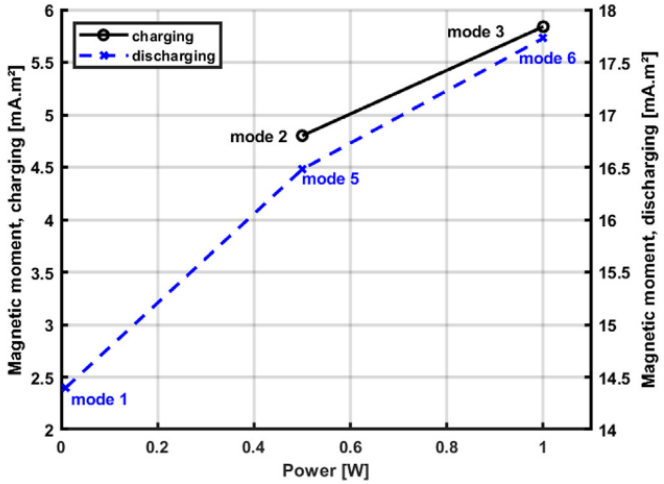

Wolfgang Treberspurg; Stren, A.; Holger Kügler; Bauer, J.; Carsten Scharlemann. Magnetic Properties of a 3U CubeSat with Electric Propulsion. *Advances in space research* **2023**, *72* (8), 3336–3343. https://doi.org/10.1016/j.asr.2023.07.002

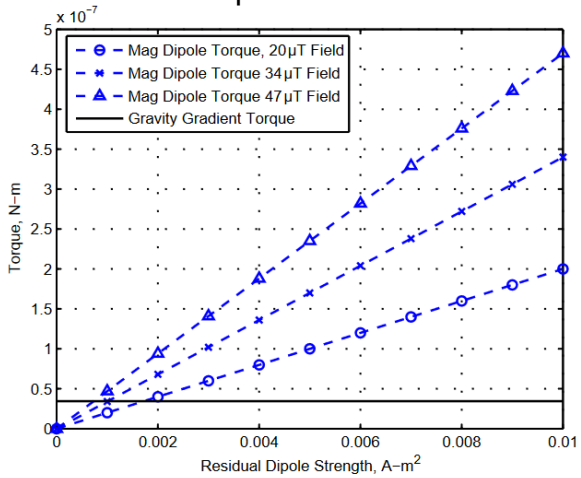

John C. Springmann, J. C., Cutler, J.W. Magnetic Sensor Calibration and Residual Dipole Characterization for Application to Nanosatellites AIAA/AAS Astrodynamics Specialist Conference. **2010**. https://doi.org/10.2514/mastro10

DC-induced fields from onboard equipment can interfere with measurement capabilities

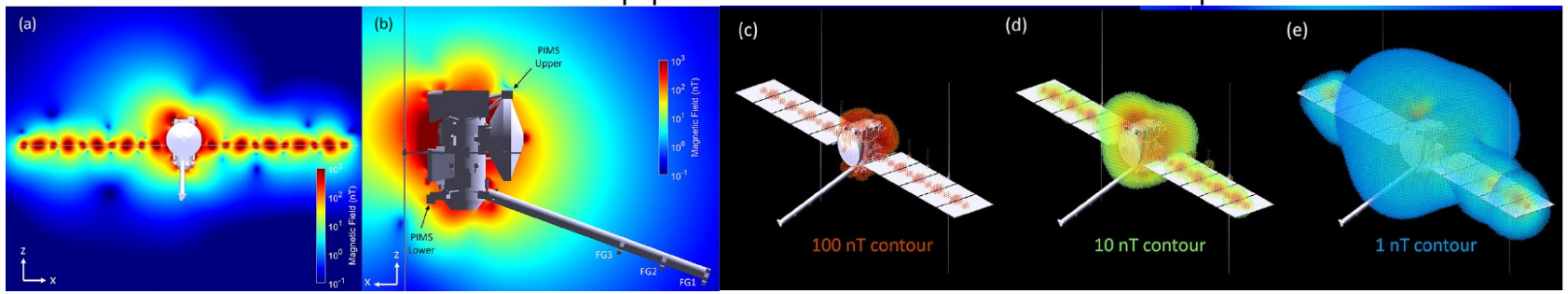

Cochrane, C. J.; Murphy, N.; Raymond, C. A.; Biersteker, J. B.; Dang, K.; Jia, X.; Korth, H.; Narvaez, P.; Ream, J. B.; Weiss, B. P. Magnetic Field Modeling and Visualization of the Europa Clipper Spacecraft. **2023**, *219* (4). https://doi.org/10.1007/s11214-023-00974-y

Magnetic fields must be accounted for and removed if possible, otherwise can interfere with attitude control and onboard equipment

Imparting magnetic cleanliness to battery cells

Pre-degaussing

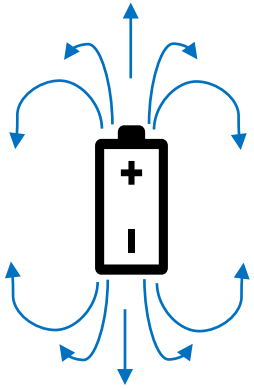

Degaussing waveform

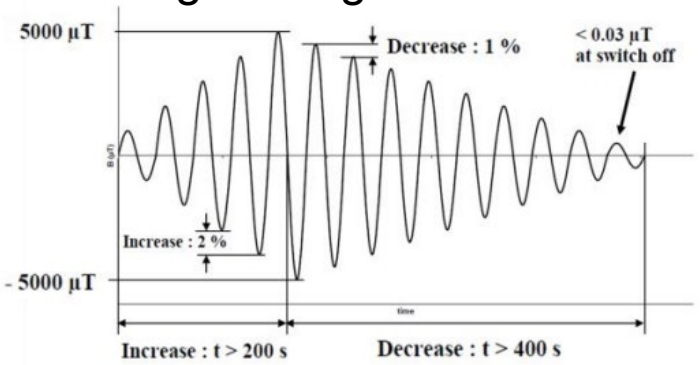

Space Engineering Electromagnetic Compatibility ECSS Secretariat ESA-ESTEC Requirements & Standards Section Noordwijk, the Netherlands; 2022.

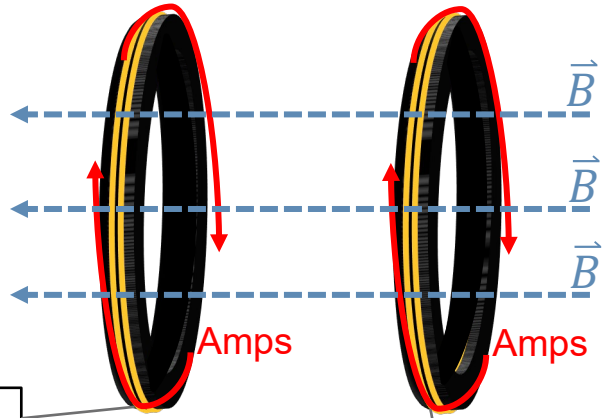

Power supply

Imparting magnetic cleanliness to battery cells

Pre-degaussing

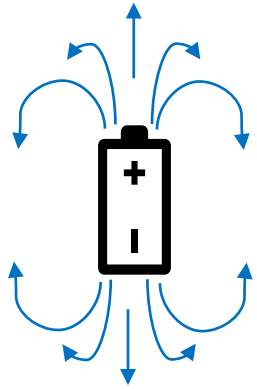

Degaussing waveform

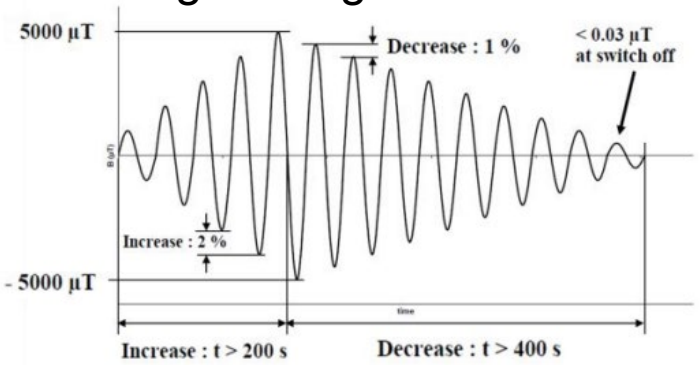

Space Engineering Electromagnetic Compatibility ECSS Secretariat ESA-ESTEC Requirements & Standards Section Noordwijk, the Netherlands; 2022.

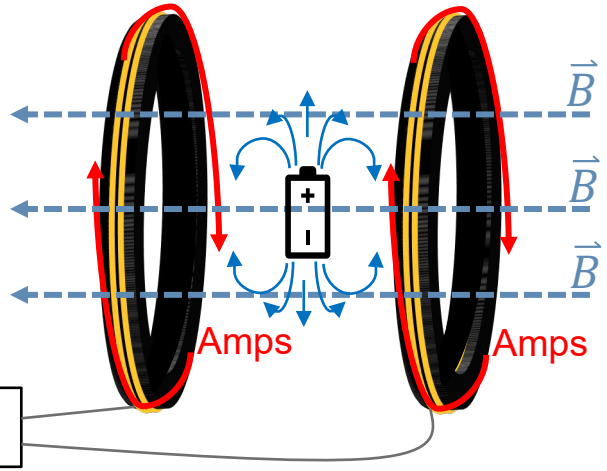

Power supply

Post-degaussing

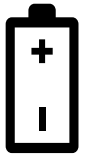

Issue of interest:

"battery cells remagnetise after several charging and discharging cycles which makes the magnetization behaviour even more unpredictable"

Arranz, C. et al. Magnetic cleanliness on NanoMagSat, a CubeSats' constellation science mission. EMC Europe 2023 - The International Symposium and Exhibition on Electromagnetic Compatibility, Sep 2023, Cracovie, Poland. ff10.1109/EMCEurope57790.2023.10274205ff. ffcea-04304164f

What does re-magnetization look like in degaussed Li-ion cells after several cycles, and how does it compare to cells with their native magnetic field (without degaussing)?

Advanced magnetic mapping methods

Rotary battery mapping system designed to measure magnetic fields

Magnetometry (TDA Safe Li⁺on)

- Gantry - Scan Resolution (X, Y, and Z): 1 mm at 0 mm standoff
- Gantry - Scanned Volume: 360°(X), 205 mm(Y), 50 mm(Z)
- Magnetometer - Sensitivity ≈ 0.3 µT
- Magnetometer - LOD ≈ 0.2 µT
- Magnetometer - LDR = ±1200 µT
- Magnetometer - Thermal Drift ≤ 0.4 µT/°C

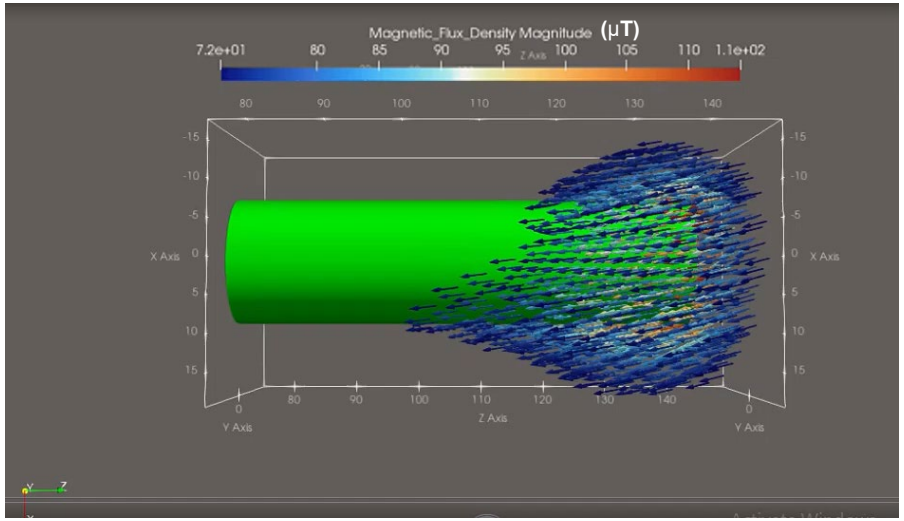

3D printed cell holder and end cap with protruded pieces to aide with battery rotation (specific to battery size)

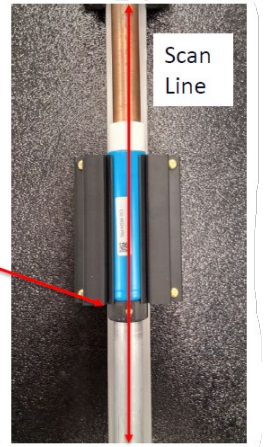

Specialized system designed for battery analysis affords high sensitivity and spatial resolution

Advanced magnetic mapping methods

Rotary battery mapping system designed to measure magnetic fields

Magnetometry (TDA Safe Li⁺on)

- Gantry - Scan Resolution (X, Y, and Z): 1 mm at 0 mm standoff
- Gantry - Scanned Volume: 360°(X), 205 mm(Y), 50 mm(Z)
- Magnetometer - Sensitivity ≈ 0.3 µT
- Magnetometer - LOD ≈ 0.2 µT
- Magnetometer - LDR = ±1200 µT
- Magnetometer - Thermal Drift ≤ 0.4 µT/°C

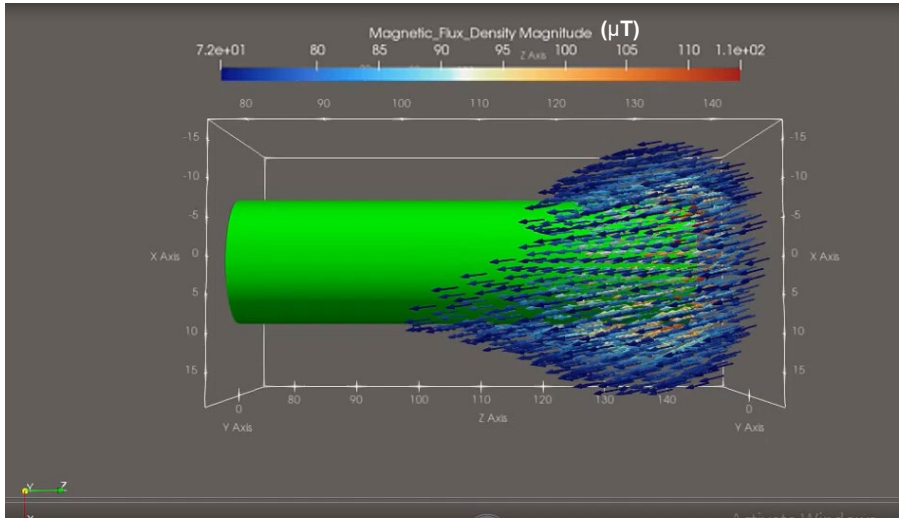

3D printed cell holder and end cap with protruded pieces to aide with battery rotation (specific to battery size)

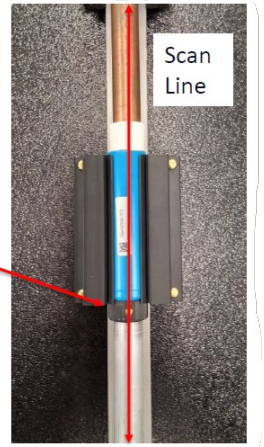

TDA RESEARCH

David Eisenberg, PhD (PI)
(Mechanical Engineering)
Non-Destructive Evaluation
Neural network construction/ implementation for large datasets

Adrienne Delluva, PhD
Materials Science
Magnetic Model of Batteries

Ellie Steward, BS
Chemical Engineering
LiB MFD Library Creation

Specialized system designed for battery analysis affords high sensitivity and spatial resolution

Experimental Details

1. **Cells of interest:**
- Moli M35A (contains graphite anode)
- **Degaussed using a Helmholtz coil, compared to cells with a native field**

2. **Characterization steps**: Initial inspection, “break-in”, fast charge/discharge

“Break-in”: C/10 cycling between 2.5→4.2V

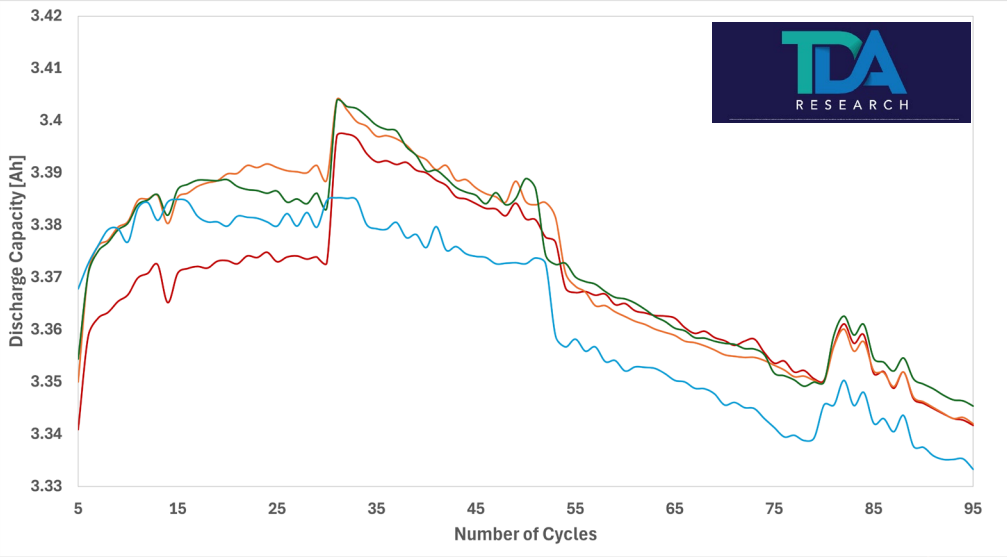

CC-CV charge (C/2→100mA cutoff), 2.3C discharge→ 90% SoH

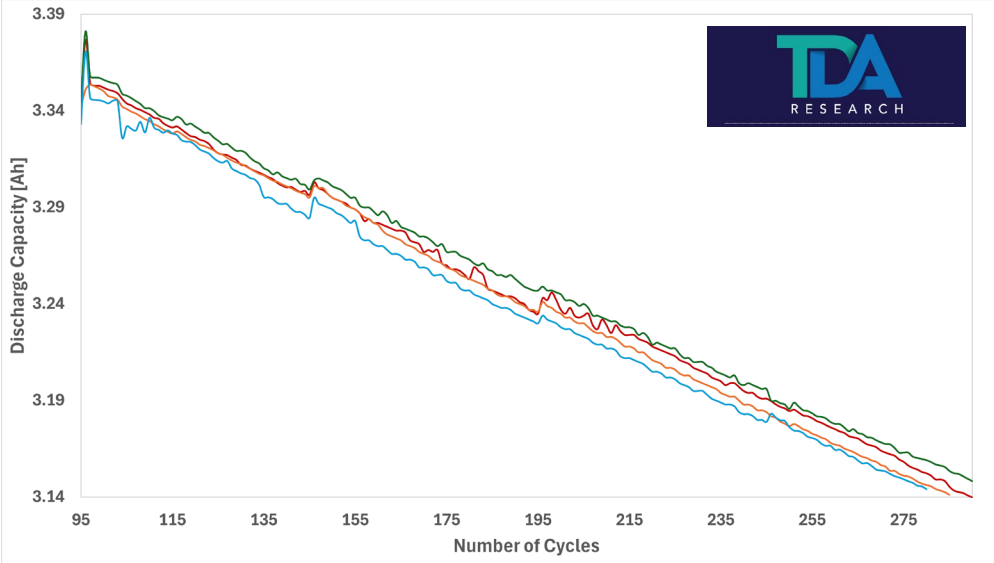

How will fields change between cells degaussed to those with their native field, at key steps in their lifetime (break in, state of health decline)?

Effect of cycling on degaussed cells

Post initial characterization

Post Break-in

↓5% State of Health

Cell 1

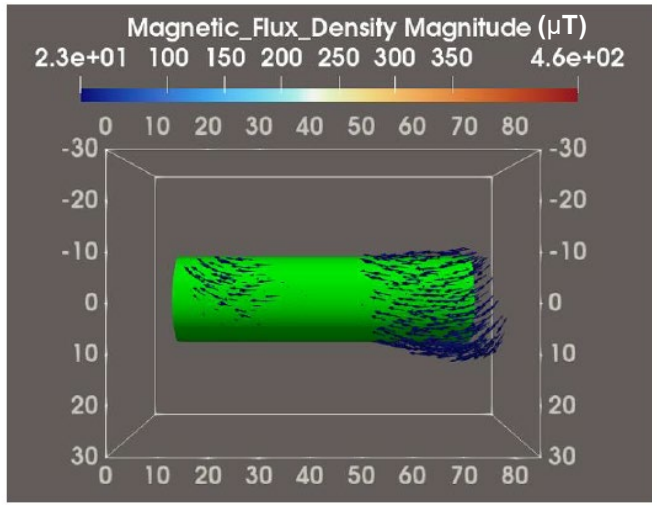

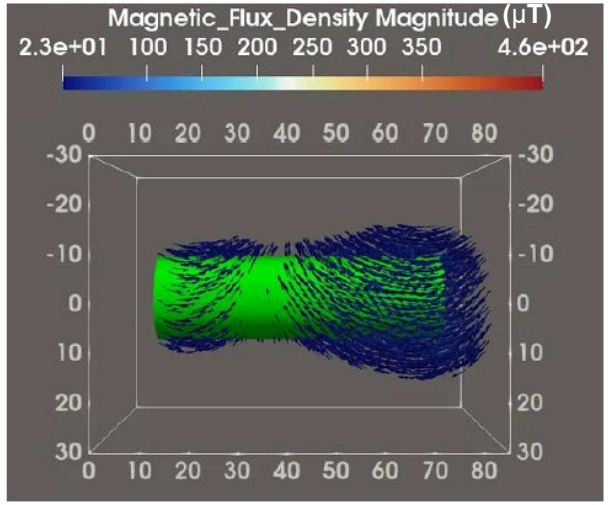

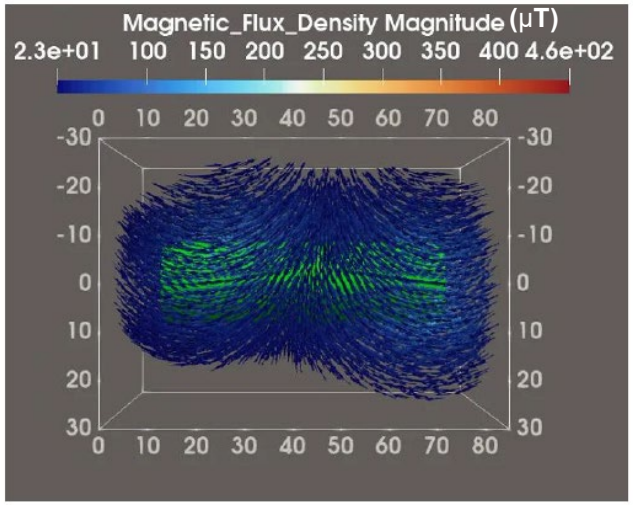

Cell orientation

Cell 2

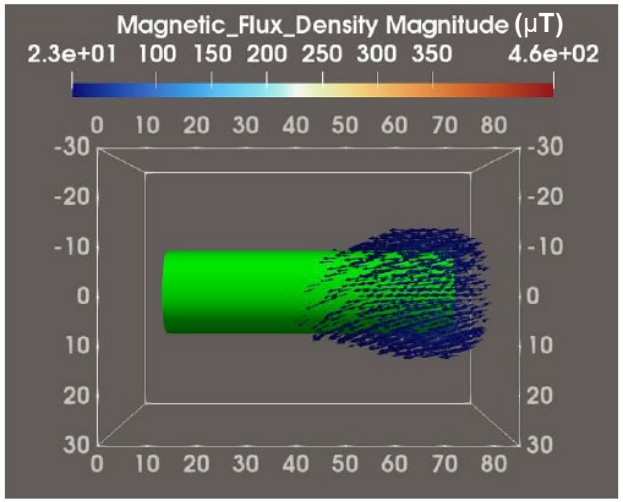

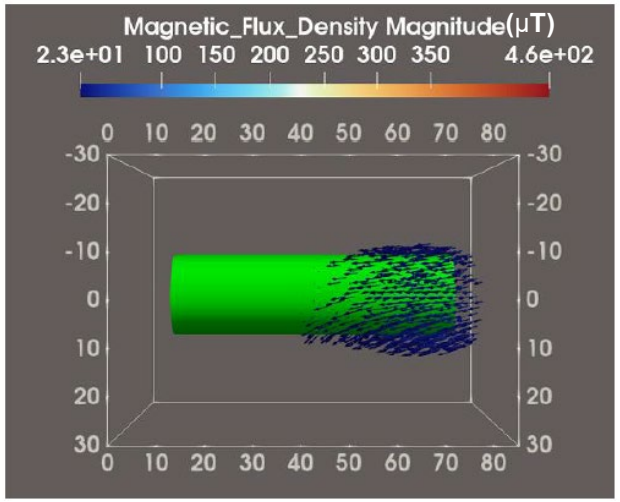

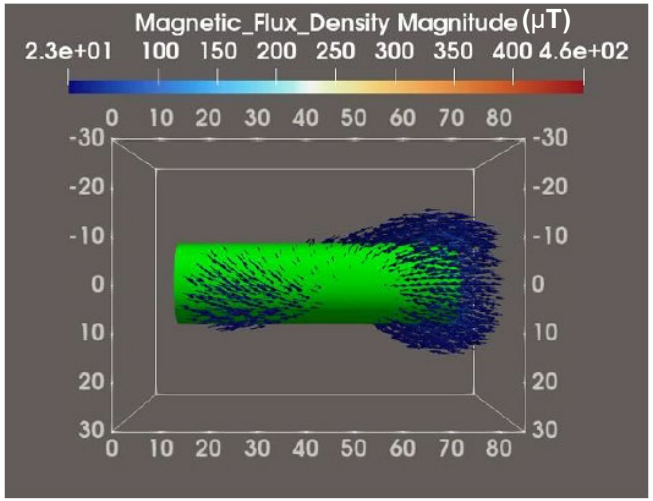

Fields migrate along length of and extend from degaussed cells; effects of degaussing are impermanent

Effect of cycling on cells with native field

Post initial characterization

Post Break-in

↓5% State of Health

Cell 3

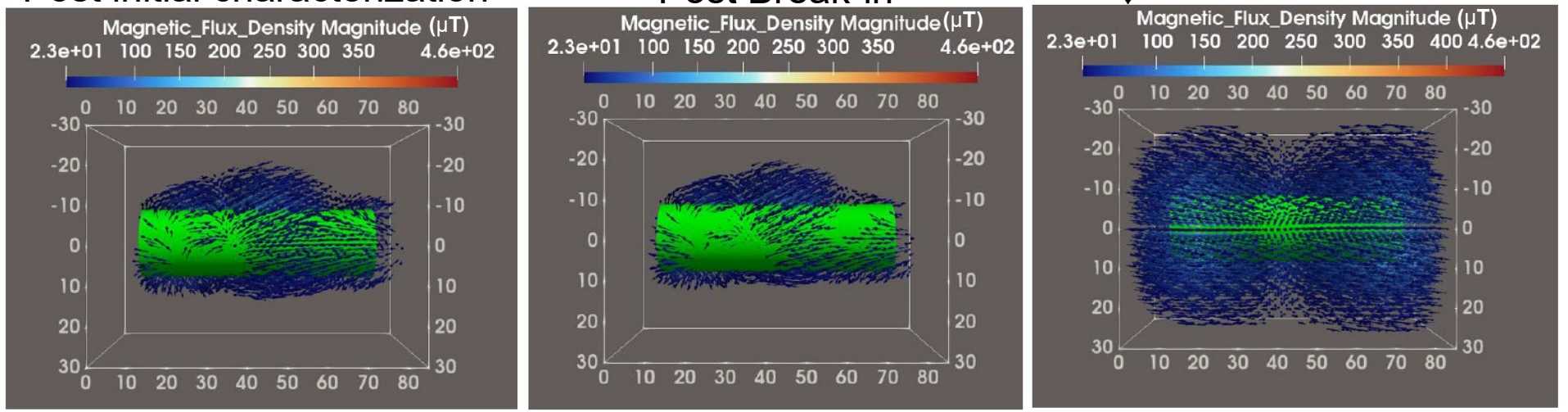

Cell orientation

Cell 4

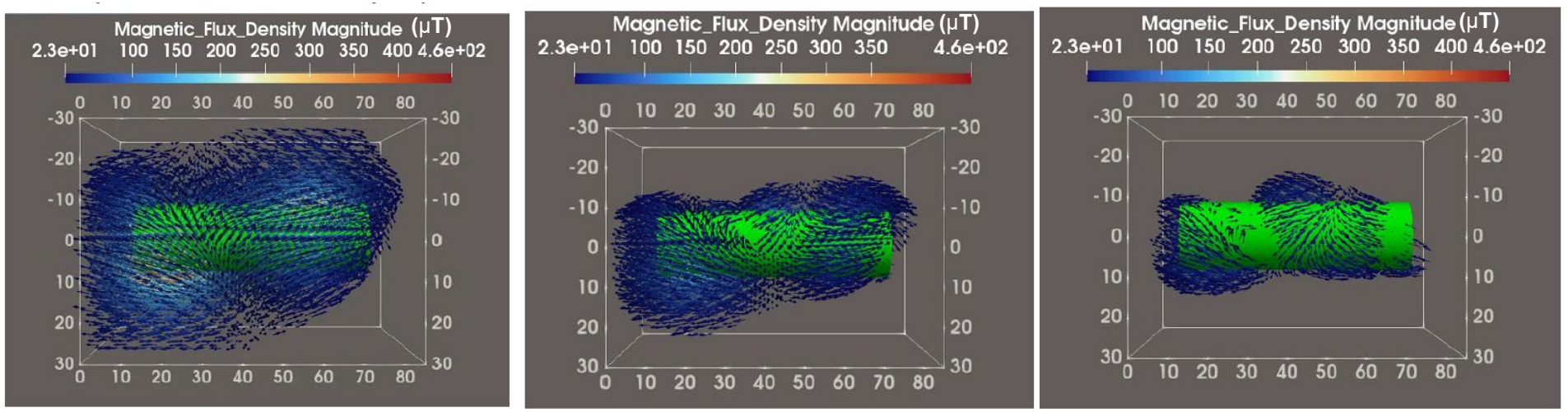

Fields follow an unpredictable pathway in cells containing their native field

Effect of cycling on cell re-magnetization

Cell orientation

Degaussed

Post initial characterization

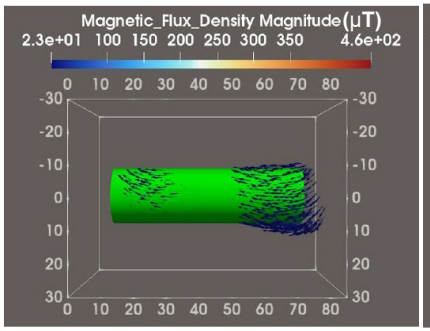

Post Break-in

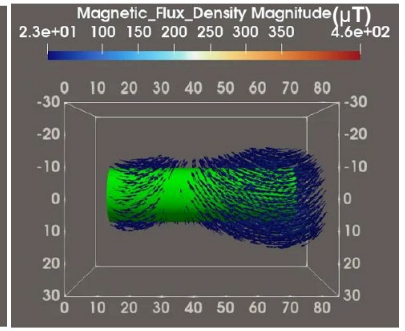

↓5% State of Health

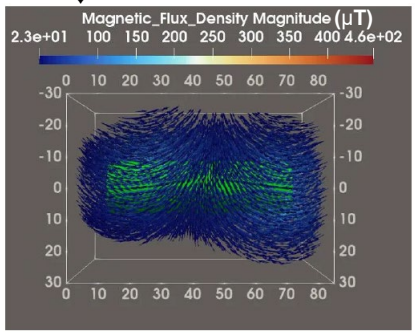

Post initial characterization

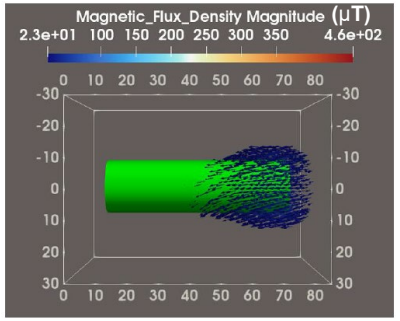

Post Break-in

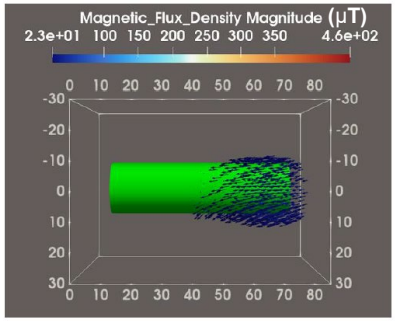

↓5% State of Health

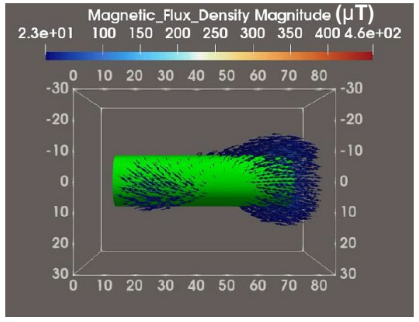

Native field

Post initial characterization

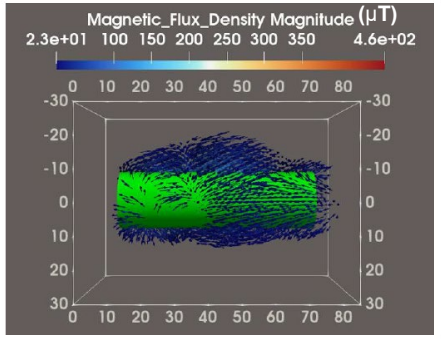

Post Break-in

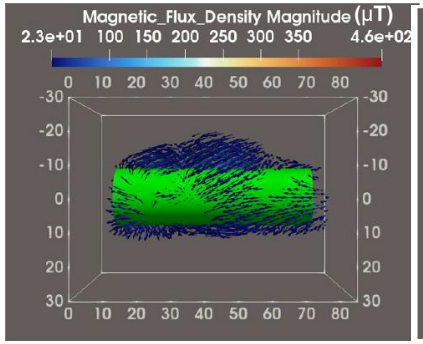

↓5% State of Health

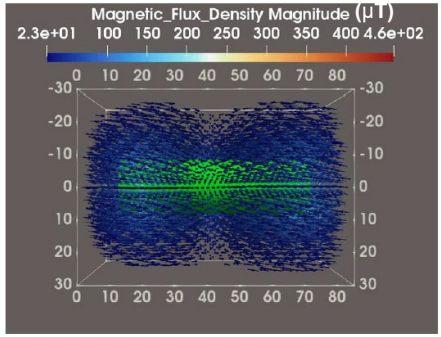

Post initial characterization

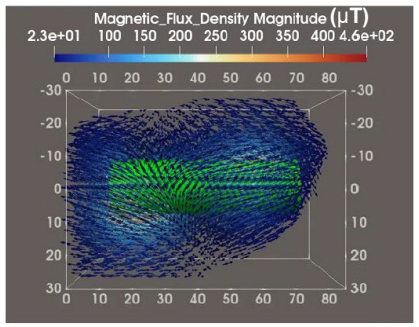

Post Break-in

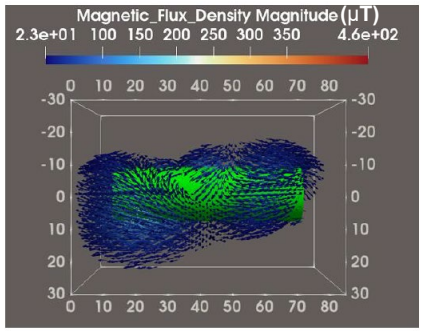

↓5% State of Health

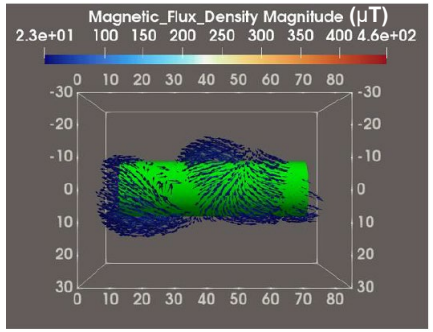

Fields migrate & grow along degaussed cells, but follow an unpredictable pathway in cells containing their native field

Conclusions, future work and opportunities

Conclusions

- Cell-specific magnetic signatures exist during electrochemical cycling (Si-containing pouch cells vs. graphite-containing cylindrical cells)
- Static magnetic fields rebuild in cells despite degaussing, while cells with a native field exhibit unpredictable evolution of magnetic signatures as a function of cycling

Future work

- Extend analysis to Si-containing cylindrical cells
- Investigate correlations between initial magnetic field magnitude and capacity degradation

Opportunities

- Potential for optimization/refinement of degaussing protocol
- Extension of magnetic mapping technique on cells paired to cancel field

Special thanks

Aerospace colleagues and TDA alumni

AEROSPACE

Michael Angell

Daniel Shoemaker

Ethan Tucker

David Hinkley

Joanna Cardema

TDA RESEARCH

Josh Biller, PhD (PI)
(Physical Chemistry)
CF electromagnetic sensors
RF testing and characterization
Electricity & Magnetism

Kevin Finch, PhD (Technical Lead)
Systematic Library Generation Software Design
Magnetic Model of Batteries


Thank you

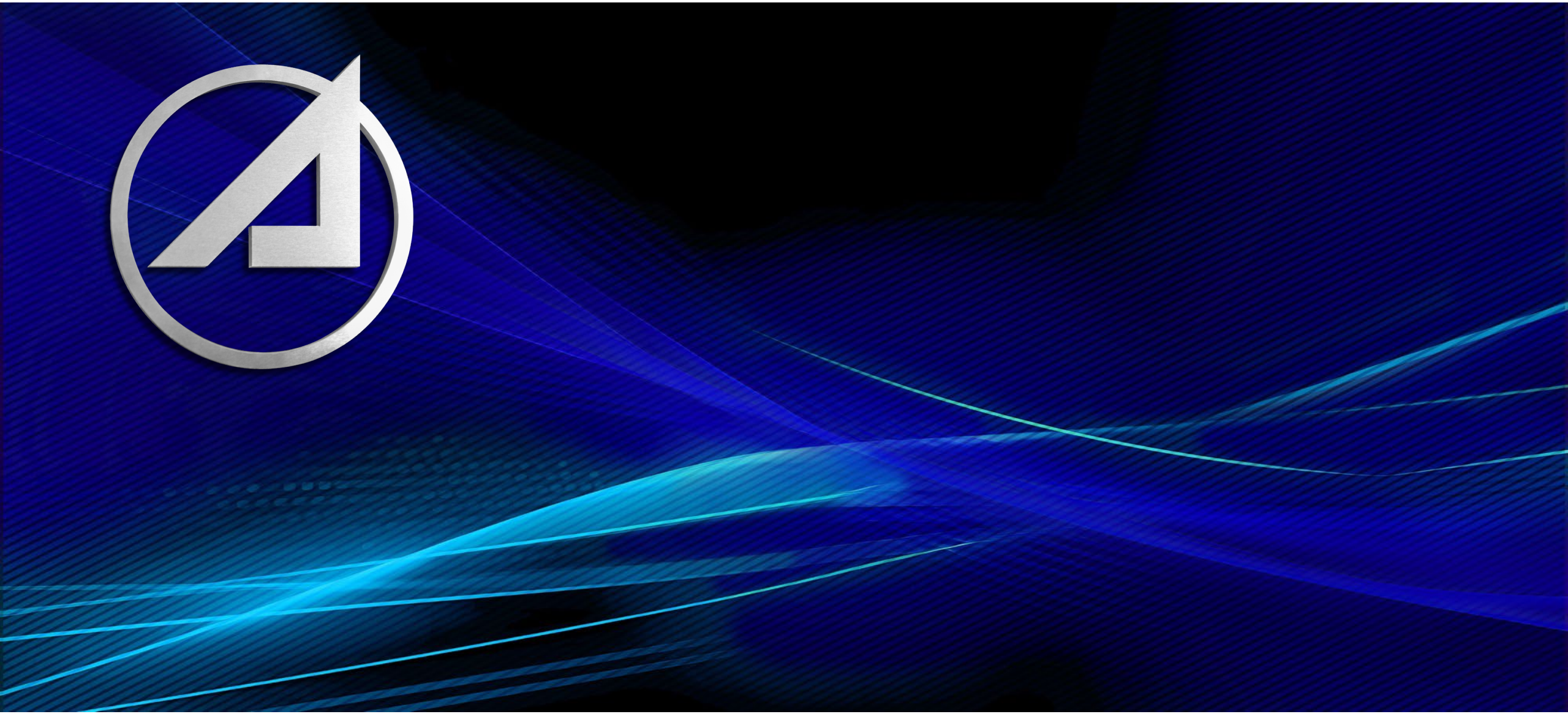

Distinguishing macroscopic and atomic-level magnetic properties within battery cells and active materials

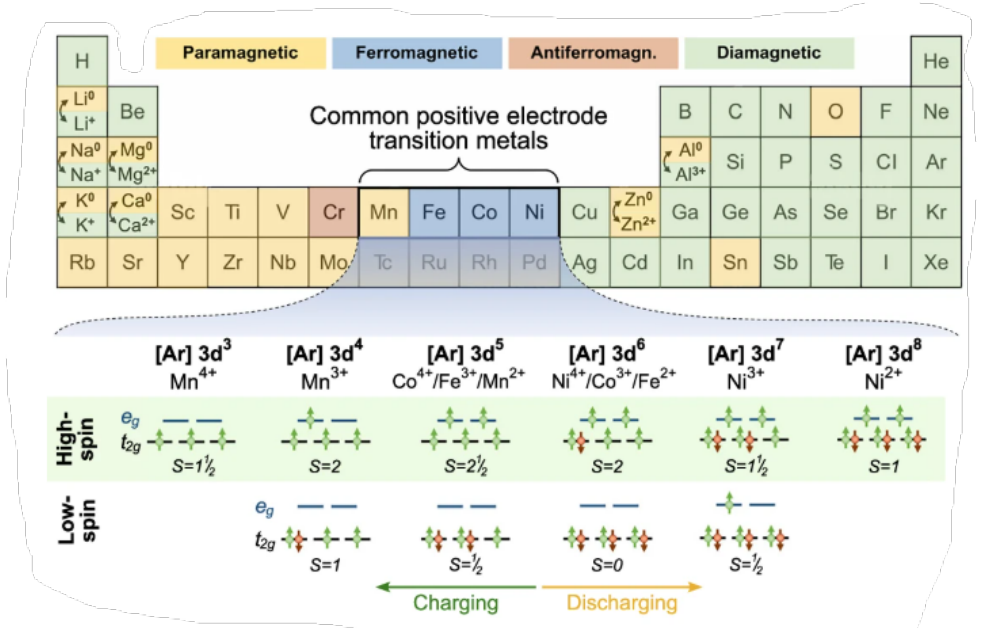

Pollok, S., Khoshkalam, M., Ghaffari-Tabrizi, F. *et al.* Magnetic microscopy for operando imaging of battery dynamics. *Nat Commun* **16**, 8303 (2025).

https://doi.org/10.1038/s41467-025-63409-y

Cycling profiles of cylindrical and pouch cells

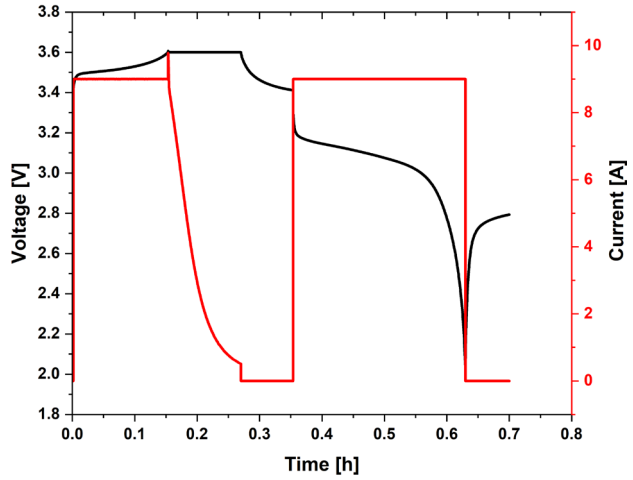

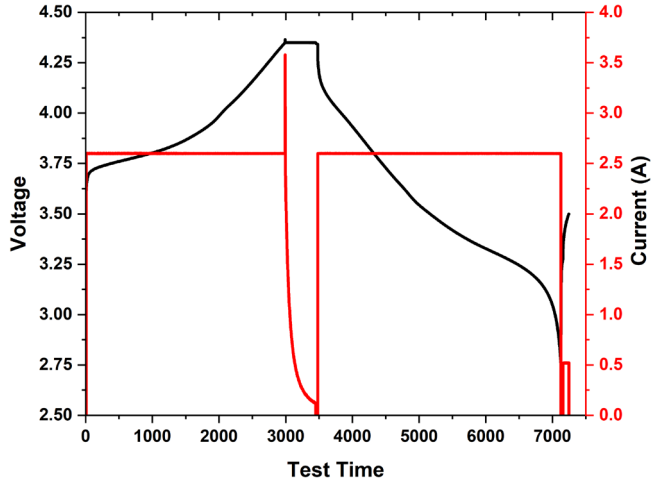

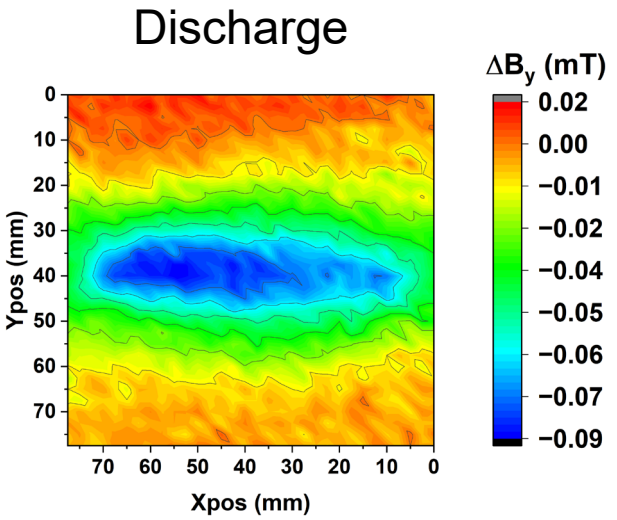

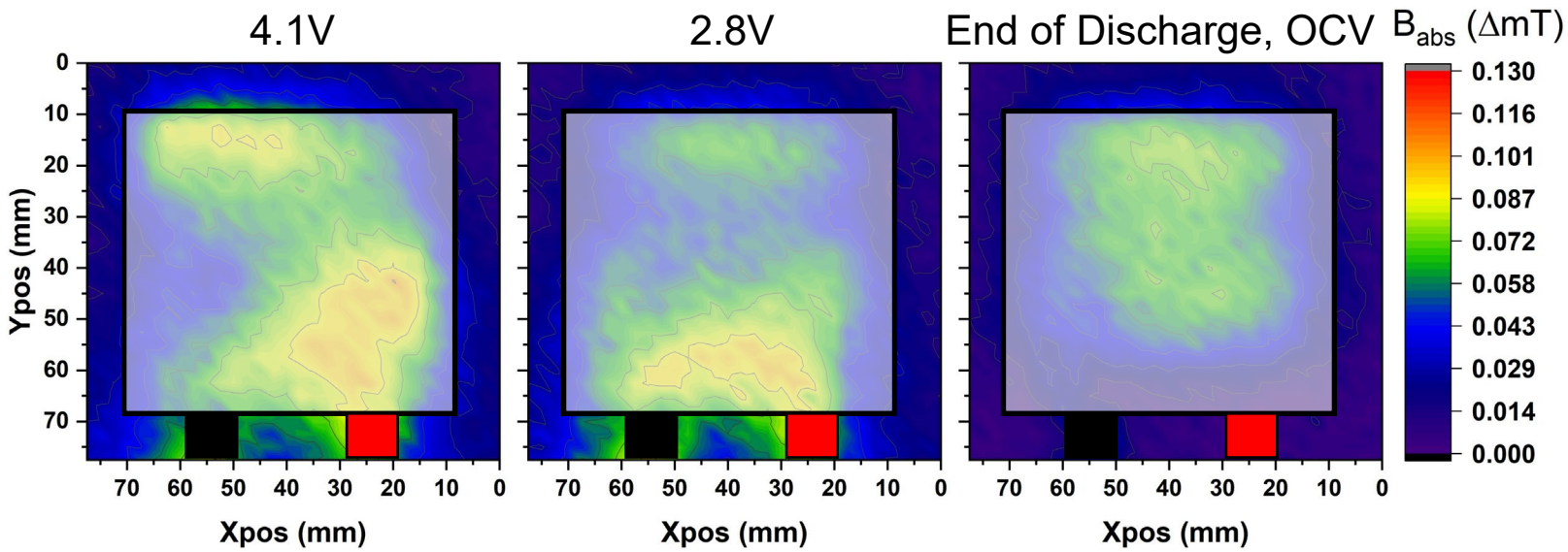

Vector-specific contributions to Si-containing cell